store-dependent Ca^{2+} influx. Such regulation is reminiscent of excitation–contraction coupling in skeletal muscle[21,22]. Like the preferred localization of ryanodine receptors in terminal cisternae[22], microdomains of highly expressed $InsP_3$ receptors next to the plasma membrane[23] may form a site of regulatory interaction between the $InsP_3$ receptors and Ca^{2+}-influx channels. Irrespective of the nature of the interaction between the channels, our findings strongly support the coupling hypothesis[2,7]. □

Methods

Cells. Control cells and clone 56 of HEK293 cells stably expressing Htrp3 (ref. 8) were grown in DMEM medium supplemented with 10% FBS, 1% penicillin/streptomycin and 200 $\mu g\,ml^{-1}$ G418 (Gibco BRL) and maintained at 37 °C in 5% CO_2. One day before the experiments, cells were transferred to glass coverslips for patch-clamp recordings.

Electrophysiology. In the cell-attached mode, the pipette solution contained 100 mM Na/HEPES and 2 mM $CaCl_2$; pH of all solutions was 7.4. Before changing to high-K^+ solution, cells were bathed in normal Ringer solution containing (in mM): 140 NaCl, 10 KCl, 1 $MgCl_2$, 2 $CaCl_2$, 10 HEPES. After a seal was established, the medium was replaced with a high-K^+ solution containing (in mM): 145 KCl, 5 NaCl, 1 $MgCl_2$, 2 $CaCl_2$, 10 HEPES. For estimation of channel permeability for Ba^{2+}, pipettes were filled with 100 mM $BaCl_2$, 10 HEPES, or 100 mM Ba^{2+}/HEPES, 2 $BaCl_2$. Patches were excised into a solution containing (in mM): 140 potassium gluconate, 10 HEPES, 2 EGTA, 1 $MgCl_2$, 5 NaCl, 1.13 $CaCl_2$ (pCa7), or a solution without $CaCl_2$. For whole-cell studies, the pipette solution contained (in mM): 120 potassium gluconate, 20 HEPES, 10 EGTA, 1 $MgCl_2$, 5 NaCl, 5 ATP. Bath solution during whole-cell experiments was normal Ringer. Current was recorded with an Axopatch 200B patch-clamp amplifier equipped with a Digidata 1200 PC interface. Currents were recorded at 2–5 kHz, filtered at 0.2–1 kHz and analysed with Axoscope 1.1, PClamp 6.0.3 (Axon Instruments) and Origin 5.0 (Microcal) software. NP_0 was determined using the following equation: $NP_0 = \langle I \rangle / i$, where $\langle I \rangle$ and i are the mean channel current and unitary current amplitude, respectively.

Cerebellar microsomes. Bovine or rat cerebella (or forebrains) were homogenized in a solution containing (in mM): 50 Tris, 100 NaCl and 2 EDTA. The homogenate was centrifuged for 10 min at 500*g* and the supernatant was collected and centrifuged for 25 min at 40,000*g*. The pellet was resuspended in the bath solution during patch-clamp experiments and stored at −80 °C.

Expression of recombinant $InsP_3R$ and preparation of proteoliposomes. COS-1 or HEK293 cells were transfected with the plasmid p$InsP_3$R-T1 (recombinant $InsP_3R$), p(1-6)$InsP_3$R-T1 ($\Delta CInsP_3R$), or salmon sperm single-stranded DNA (control in Fig. 6g) as described in ref. 24. Cells were collected 48–72 h post-transfection and microsomes were prepared as described[24]. Microsomes from control and $InsP_3$R1-expressing cells were solubilized in 1% CHAPS buffer and fractionated through 5–20% sucrose (w/v) gradients. Gradient fractions containing $InsP_3R$ were identified by immunoblotting with $InsP_3$R1-specific antibody. Fresh $InsP_3R$ fractions and parallel fractions of control cells were reconstituted into liposomes as described[25]. Proteoliposomes from cells transfected with p$InsP_3$R-T1 yielded pronounced channel activity when incorporated into lipid bilayers, and those containing the COS-1 control had no channel activity (data not shown). HEK293 cells expressing $\Delta CInsP_3R1$ were used to prepare microsomes by the procedure already described for the preparation of cerebellar microsomes.

Received 20 August; accepted 8 October 1998.

1. Putney, J. W. J. & Bird, G. S. J. The inositol phosphate–calcium signaling system in nonexcitable cells. *Endocr. Rev.* **14,** 610–631 (1993).
2. Berridge, M. J. Capacitative calcium entry. *Biochem. J.* **312,** 1–11 (1995).
3. Parech, A. B. & Penner, R. Store depletion and calcium influx. *Physiol. Rev.* **77,** 901–930 (1997).
4. Hoth, M. & Penner, R. Depletion of intracellular calcium stores activates a calcium current in mast cells. *Nature* **355,** 353–356 (1990).
5. Zweifach, A. & Lewis, R. S. Mitogen-regulated Ca^{2+} current of T lymphocytes is activated by depletion of intracellular Ca^{2+} stores. *Proc. Natl Acad. Sci. USA* **90,** 6295–6299 (1993).
6. Randriamampita, C. & Tsien, R. Y. Emptying of intracellular Ca^{2+} stores releases a novel small messenger that stimulates Ca^{2+} influx. *Nature* **364,** 809–814 (1993).
7. Irvine, R. F. 'Quantal' Ca^{2+} release and the control of Ca^{2+} entry by inositol phosphates—a possible mechanism. *FEBS Lett.* **263,** 5–9 (1990).
8. Zhu, X. *et al. trp*, a novel mammalian gene family essential for agonist-activated capacitative Ca^{2+} entry. *Cell* **58,** 661–671 (1996).
9. Hurst, R. S., Zhu, X., Boulay, G., Birnbaumer, L. & Stefani, E. Ionic currents underlying Htrp3 mediated agonist-dependent Ca^{2+} influx in stably transfected HEK293 cells. *FEBS Lett.* **422,** 333–338 (1998).
10. Kiselyov, K. I., Mamin, A. G., Semyonova, S. B. & Mozhayeva, G. N. Low-conductance high selective inositol (1,4,5)-trisphosphate activated Ca^{2+} channels in plasma membrane of A431 cells. *FEBS Lett.* **407,** 309–312 (1997).
11. Kiselyov, K. I., Semyonova, S. B., Mamin, A. G. & Mozhayeva, G. N. Miniature Ca^{2+} channels in plasma membrane excised patches: activation by IP_3 receptor. *Pfluegers Arch* (in the press).
12. Zitt, C. *et al.* Cloning and functional expression of a human Ca^{2+}-permeable cation channel activated by calcium store depletion. *Neuron* **138,** 1333–1341 (1997).
13. Zitt, C. *et al.* Expression of TRPC3 in Chinese hamster ovary cells results in calcium-activated cation currents not related to store depletion. *J. Cell Biol.* **138,** 1333–1341 (1997).
14. Merritt, J. E. *et al.* SK&F 96365, a novel inhibitor of receptor-mediated calcium entry. *Biochem. J.* **271,** 515–522 (1990).
15. Zhu, X., Jiang, M. & Birnbaumer, L. Receptor-activated Ca^{2+} influx via human Trp3 stably expressed in human embryonic kidney (HEK)293 cells. Evidence for a non-capacitative Ca^{2+} entry. *J. Biol. Chem.* **273,** 133–142 (1998).
16. Gafni, J. *et al.* Xestospongins, potent membrane permeable blockers of the inositol 1,4,5-trisphosphate receptor. *Neuron* **19,** 723–733 (1997).
17. Takemura, H., Hughes, A. R., Thastrup, O. & Putney, J. W. J. Activation of calcium entry by the tumor promoter thapsigargin in parotid acinar cells. *J. Biol. Chem.* **264,** 12266–12271 (1989).
18. Smith, P. M. & Gallacher, D. V. Thapsigargin-induced Ca^{2+} mobilization in acutely isolated mouse lacrimar cells is dependent on a basal level of IP_3 and is inhibited by heparin. *Biochem. J.* **229,** 37–40 (1994).
19. Sharp, A. H. *et al.* Differential immunohistochemical localization of inositol 1,4,5-trisphosphate- and ryanodine-sensitive Ca^{2+} release channels in rat brain. *J. Neurosci.* **13,** 3051–3063 (1993).
20. Sugawara, H., Kurosaki, M., Takata, M. & Kurosaki, T. Genetic evidence for involvement of type 1, type 2 and type 3 inositol 1,4,5-trisphosphate receptors in signal transduction through the B-cell antigen receptor. *EMBO J.* **16,** 3078–3088 (1997).
21. Beam, K. G. & Franzini-Armstrong, C. Functional and structural approaches to the study of excitation–contraction coupling. *Meth. Cell Biol.* **52,** 283–306 (1997).
22. Franzini-Armstrong, C. & Jorgensen, A. O. Structure and development of E–C coupling units in skeletal muscle. *Annu. Rev. Physiol.* **56,** 509–534 (1994).
23. Muallem, S. & Lee, M. G. High $[Ca^{2+}]_i$ domains, secretory granules and exocytosis. *Cell Calcium* **22,** 1–4 (1997).
24. Mignery, G. A., Newton, C. L., Archer III, B. T. & Sudhof, T. C. Structure and expression of the rat inositol 1,4,5-trisphosphate receptor. *J. Biol. Chem.* **265,** 12579–12685 (1990).
25. Ramos-Franco, J., Caenepeel, S., Fill, M. & Mignery, G. A. A single channel function of recombinant type-1 inositol 1,4,5-trisphosphate receptor ligand binding domain splice variants. *Biophys. J.* (in the press).
26. Lee, M. G. *et al.* Polarized expression of Ca^{2+} channels in pancreatic and salivary cells. Correlation with initiation and propagation of $[Ca^{2+}]_i$ waves. *J. Biol. Chem.* **272,** 15765–15770 (1997).

Acknowledgements. We thank I. Bezprozvanny for insightful discussions. This work was supported by the NIH.

Correspondence and requests for materials should be addressed to S.M. (e-mail: smuall@mednet.swmed.edu).

The receptor Msn5 exports the phosphorylated transcription factor Pho4 out of the nucleus

Arie Kaffman, Nicole Miller Rank, Elizabeth M. O'Neill, Linda S. Huang & Erin K. O'Shea

Department of Biochemistry and Biophysics, University of California at San Francisco, School of Medicine, San Francisco, California 94143-0448, USA

The movement of many transcription factors, kinases and replication factors between the nucleus and cytoplasm is important in regulating their activity[1]. In some cases, phosphorylation of a protein regulates its entry into the nucleus[2]; in others, it causes the protein to be exported to the cytoplasm[3–6]. The mechanism by which phosphorylation promotes protein export from the nucleus is poorly understood. Here we investigate how the export of the yeast transcription factor Pho4 is regulated in response to changes in phosphate availability. We show that phosphorylation of Pho4 by a nuclear complex of a cyclin with a cyclin-dependent kinase, Pho80–Pho85, triggers its export from the nucleus. We also find that the shuttling receptor used by Pho4 for nuclear export is the importin-β-family member Msn5 (refs 7, 8), which is required for nuclear export of Pho4 *in vivo* and binds only to phosphorylated Pho4 in the presence of the GTP-bound form of yeast Ran *in vitro*. Our results reveal a simple mechanism by which phosphorylation can control the nuclear export of a protein.

When yeast are grown in phosphate-rich medium, the transcription factor Pho4 is phosphorylated by the Pho80–Pho85 cyclin–cyclin-dependent kinase (CDK) complex[9] and is localized to the cytoplasm[10], thereby turning off transcription of genes that are turned on specifi-

cally by phosphate starvation[11]. When yeast are starved of phosphate, the CDK inhibitor Pho81 inactivates Pho80–Pho85 (refs 12, 13), and Pho4 is not phosphorylated. Unphosphorylated Pho4, but not phosphorylated Pho4, is recognized by the non-classical import receptor Pse1/Kap121, indicating that nuclear import of Pho4 may be regulated in response to phosphate availability[14].

For several reasons the regulation of Pho4 import alone is unlikely to be sufficient to account for the change in Pho4 localization that is induced by phosphorylation. First, the Pho80–Pho85 cyclin–CDK complex localizes to the nucleus (Fig. 1a), whereas phosphorylated Pho4 is cytoplasmic[10]. These observations indicate that Pho4 may be phosphorylated in the nucleus and exported to the cytoplasm.

Second, we observed that phosphorylated Pho4 was rapidly exported from the nucleus. To monitor export of Pho4, we first grew a yeast strain expressing a fusion of Pho4 and green fluorescent protein (GFP) in medium lacking phosphate; this led to accumulation of unphosphorylated Pho4–GFP in the nucleus (Fig. 1b, top). We added cycloheximide to prevent further protein synthesis. We then added phosphate to activate the Pho80–Pho85 kinase, and monitored the localization of Pho4–GFP. After 3–6 min the localization of Pho4–GFP was indistinguishable from that seen in cells grown in phosphate-rich medium (Fig. 1b, top). If no phosphate was added to the culture, Pho4–GFP remained in the nucleus for several hours (data not shown). An alternative explanation for these results, that phosphorylation of Pho4–GFP leads to degradation of nuclear Pho4–GFP followed by cytoplasmic accumulation of newly synthesized protein, is unlikely because protein synthesis was inhibited. To test the role of phosphorylation in the rapid export of Pho4, we studied the export of $Pho4^{SA}$, a mutant Pho4 containing five serine-to-alanine substitutions at the sites of phosphorylation by Pho80–Pho85 (ref. 10). $Pho4^{SA}$ did not leave the nucleus upon addition of phosphate to a starved culture of yeast (Fig. 1b, bottom). In addition, in strains lacking either the cyclin Pho80 or the CDK Pho85, Pho4–GFP did not leave the nucleus upon addition of phosphate (data not shown). These data indicate that phosphorylation of Pho4 is required for its cytoplasmic accumulation.

To determine whether the export of Pho4 from the nucleus is regulated by phosphorylation, it is necessary to examine export in the absence of import[15]. If the export of Pho4 is enhanced by phosphorylation, phosphorylated Pho4 will accumulate in the cytoplasm more rapidly than unphosphorylated Pho4 when import is blocked. In contrast, if the export of Pho4 is not regulated by phosphorylation, both forms of Pho4 will accumulate in the cytoplasm at the same rate when import is blocked (Fig. 2a).

We first demonstrated that two temperature-sensitive yeast mutants with a conditional defect in protein import, *nsp1*^{ts} (refs 16, 17) and *nup49-313* (refs 16, 18), were defective for import of Pho4 when grown at the restrictive temperature (data not shown). An experiment using the *nsp1*^{ts} strain expressing Pho4–GFP was performed as follows (Fig. 2b, top). First, the yeast were starved for phosphate at 23 °C, allowing unphosphorylated Pho4–GFP to accumulate in the nucleus. The culture was then shifted to 38.5 °C to impair protein import, treated with cycloheximide and split in half. Phosphate was added to half of the culture to activate Pho80–Pho85 and trigger phosphorylation of Pho4, and was not added to the other half. Pho4–GFP was rapidly transported to the cytoplasm in the culture to which phosphate had been added, whereas it remained nuclear in the untreated culture for several more hours (Fig. 2b, bottom). In addition, when phosphate was added, $Pho4^{SA}$ remained in the nucleus for several hours when import was blocked (data not shown). These data indicate that phosphorylation may regulate nuclear export of Pho4.

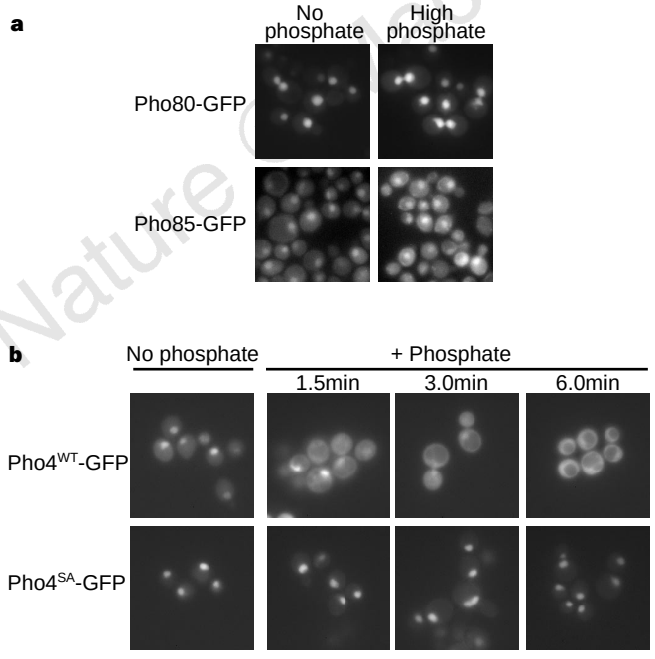

Figure 1 Phosphorylation of Pho4 by nuclear Pho80–Pho85 promotes its rapid export from the nucleus. **a**, Direct fluorescence microscopy of cells carrying a plasmid expressing Pho80–GFP or Pho85–GFP grown in high- or no-phosphate media. As both Pho80 and Pho85 are required to phosphorylate Pho4 (ref. 9), the localization of Pho80 restricts the kinase activity to the nucleus. **b**, Fluorescence microscopy of cells carrying a plasmid expressing $Pho4^{WT}$–GFP or $Pho4^{SA}$–GFP (a non-phosphorylatable mutant) under the control of the *PHO4* promoter. Cells were starved of phosphate (no phosphate) and incubated with cycloheximide for 10 min. At $t = 0$ min phosphate was added to the culture and localization of Pho4–GFP was monitored as a function of time.

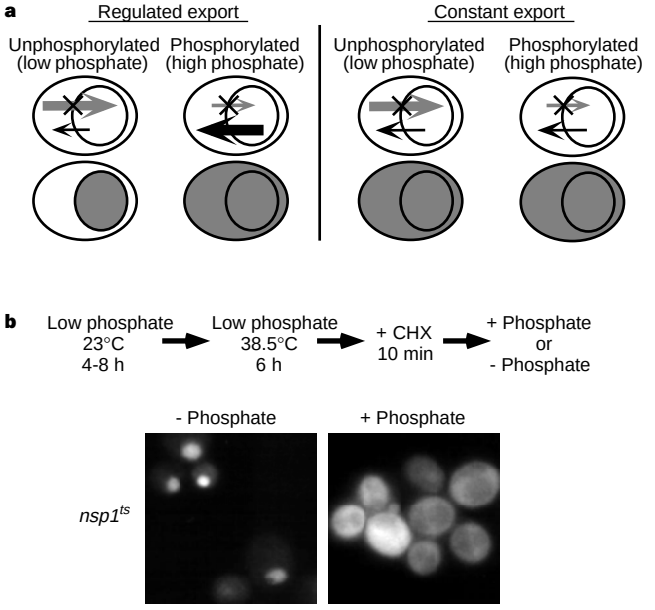

Figure 2 The rate of export of Pho4 from the nucleus is regulated by phosphorylation. **a**, Predicted outcomes of blocking import when export is either regulated or is constant. **b**, Top, outline of the experiment used to determine whether the rate of export is regulated in response to phosphorylation; CHX, cycloheximide. Bottom, localization of $Pho4^{WT}$–GFP in an *nsp1*^{ts} strain[16,17] that has been starved of phosphate and incubated in cycloheximide at 38.5 °C. The culture was split and phosphate was added to half of the culture (+ Phosphate) but not to the other half (– Phosphate). The addition of phosphate to the *nsp1*^{ts} strain resulted in export of Pho4–GFP with the same kinetics as seen in the wild-type strain.

To understand the molecular mechanism by which phosphorylation regulates Pho4 export, we wished to identify the Pho4 export receptor. We therefore studied the localization of Pho4–GFP in yeast strains containing mutations in putative receptors involved in nuclear transport. Thirteen proteins in yeast have homology to importin-β, a receptor that recognizes nuclear-localization signals (NLSs) on proteins imported into the nucleus[7,8]. Some importin-β-family members are transport receptors; others have not yet been characterized. No defect in Pho4 export was observed in yeast strains containing mutations in the importin-β-family members Kap104 (ref. 19), Cse1 (ref. 20), Xpo1 (ref. 21), Sxm1 (ref. 22), Kap123 (refs 22, 23) and Mtr10 (ref. 24). However, in a strain lacking the importin-β-family member Msn5/Ste21, Pho4–GFP could not be exported and was localized constitutively to the nucleus (Fig. 3a). The defect in Pho4 localization in the *msn5Δ* strain is not an indirect result of a defect in the phosphate signal-transduction pathway, as Pho4 is still phosphorylated normally in this strain (Fig. 3b). Although Pho4–GFP was localized to the nucleus in the *msn5Δ* strain, expression of the secreted acid phosphatase Pho5, which is activated by Pho4 under conditions of phosphate starvation, was not induced because there are extra mechanisms for regulating the transcriptional activity of Pho4 (E.K.O. *et al.*, manuscript in preparation).

One model that may explain regulated export of Pho4 is that Msn5 preferentially binds the phosphorylated form of Pho4. We tested this hypothesis by performing an *in vitro* binding experiment. As all protein-export pathways characterized so far require the small GTPase Ran in the GTP-bound state[25–28], we tested whether Ran–GTP is required for Msn5 to bind Pho4. Phosphorylated Pho4 bound to Msn5 in yeast extract when a Ran mutant was added that is locked in the GTP-bound state (human RanQ69L–GTP)[29] (Fig. 4a, top, lane 1). In the absence of RanQ69L–GTP, no interaction was observed between phosphorylated Pho4 and Msn5 (Fig. 4a, top, lane 2). Pho4 must be phosphorylated to interact with Msn5, as, even in the presence of RanQ69L–GTP, no interaction was seen between Msn5 and the mutant Pho4^{SA}, which cannot be phosphorylated (Fig. 4a, top, lane 3).

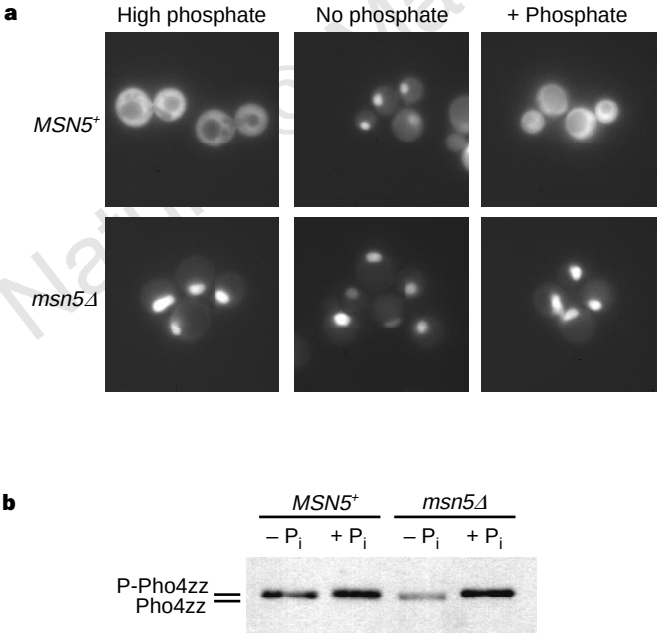

Figure 3 Msn5 is required for export of Pho4. **a**, Localization of Pho4^{WT}–GFP in wild-type (*MSN5*$^+$) and *msn5Δ* strains grown in high-phosphate medium or no-phosphate medium or 10 min after the addition of phosphate to phosphate-starved cells (+ Phosphate). **b**, Immunoblot detecting phosphorylation of Pho4^{WT}–zz in extracts from *MSN5*$^+$ and *msn5Δ* strains. Yeast strains were grown in low-phosphate medium, and phosphate was either added (+ P_i) or not added (– P_i) to the culture. Addition of phosphate to *MSN5*$^+$ and *msn5Δ* strains expressing Pho4^{WT}–zz grown in phosphate-depleted medium resulted in a shift in the electrophoretic mobility of Pho4, indicating that Pho4 was phosphorylated (P-Pho4zz)[9].

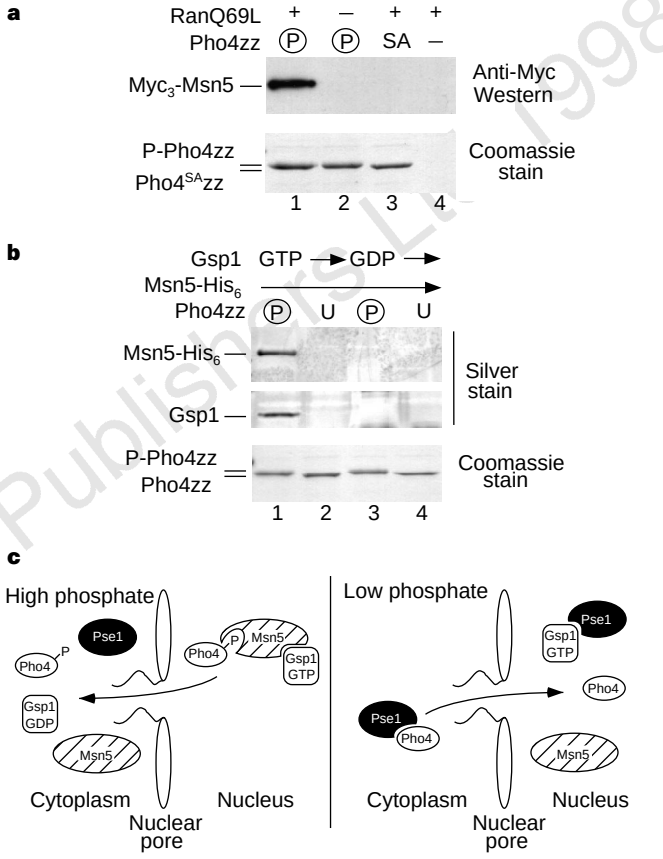

Figure 4 Msn5 binds directly to phosphorylated Pho4 in the presence of Ran-GTP. **a**, *In vitro*-phosphorylated Pho4^{WT}–zz (circ P) or Pho4^{SA}–zz (SA) or a no Pho4 control (–) was purified using IgG–Sepharose beads, and incubated with extract containing Myc_3-tagged Msn5 in the presence or absence of RanQ69L (ref. 29). Top, bound proteins were eluted with 1 M $MgCl_2$, concentrated using methanol–chloroform precipitation, separated on 7.8% SDS–PAGE and immunoblotted with anti-Myc antibodies. Lane 1, phosphorylated Pho4^{WT}–zz (P-Pho4zz) with RanQ69L; lane 2, phosphorylated Pho4^{WT}-zz without RanQ69L; lane 3, phosphorylated Pho4^{SA}–zz with RanQ69L; lane 4, beads alone with RanQ69L (lane 4). Bottom, to ensure that the same amounts of Pho4–zz were immobilized on IgG–Sepharose in the lanes shown in the top panel, Pho4–zz was eluted with 0.5 M acetic acid, pH 3.4, separated on 7.8% SDS–PAGE, and visualized with Coomassie blue. Lanes are as described above. **b**, Pho4^{WT}–zz was phosphorylated (circled P) or mock-phosphorylated (U) *in vitro*, and purified using IgG–Sepharose beads. Immobilized proteins were incubated with 1 μM purified Msn5–His_6 in the presence of 1 μM purified Myc–Gsp1 loaded with either GTP or GDP. Top, bound proteins were eluted with 1 M $MgCl_2$, concentrated using methanol–chloroform precipitation, separated on 7.8% SDS–PAGE and visualized with silver straining. Lane 1, phosphorylated Pho4^{WT}–zz with Myc–Gsp1 loaded with GTP; lane 2, unphosphorylated Pho4^{WT}–zz with Myc–Gsp1 loaded with GTP; lane 3, phosphorylated Pho4^{WT}–zz with Myc–Gsp1 loaded with GDP; lane 4, unphosphorylated Pho4^{WT}–zz with Myc–Gsp1 loaded with GDP. Roughly 20% of the Msn5–His_6 bound to phosphorylated Pho4 in the presence of Gsp1–GTP. Bottom, to ensure that the amount of Pho4–zz immobilized on IgG–Sepharose did not vary between lanes, Pho4^{WT}–zz was eluted with 0.5 M acetic acid, pH 3.4, separated on 7.8% SDS–PAGE, and visualized with Coomassie blue. Lanes are as described above. **c**, Model for the regulated nucleocytoplasmic localization of Pho4 in response to extracellular phosphate.

There are several models that could explain the preferential binding of Msn5 to phosphorylated Pho4. Preferential binding might require an adapter protein to enable the interaction with phosphorylated Pho4, or a protein that masks the Msn5-binding site on unphosphorylated Pho4, or it might be a direct consequence of the ability of Msn5 to distinguish between the two forms of Pho4. To determine whether Msn5 alone can bind preferentially to the phosphorylated form of Pho4, we used purified recombinant proteins to test the binding of Pho4 to Msn5 and the yeast Ran homologue Gsp1. Purified Msn5 bound preferentially to phosphorylated Pho4 in the presence of Gsp1 loaded with GTP (Fig. 4b, top, lane 1), but not when Gsp1 was loaded with GDP (Fig. 4b, top, lane 3). Purified Msn5 did not interact with unphosphorylated Pho4, even in the presence of Gsp1–GTP (Fig. 4b, top, lane 2). These data indicate that no additional proteins are required for Msn5 to bind preferentially to phosphorylated Pho4 and Gsp1, and that the interaction between Pho4 and Msn5 requires Gsp1–GTP. The observation that Gsp1–GTP bound to Pho4 in the presence of Msn5 (Fig. 4b, middle) but not in its absence (data not shown) indicates that phosphorylated Pho4, Gsp1–GTP and Msn5 may form a ternary complex. These results are consistent with the properties of other characterized complexes of export receptor and cargo, which require the export receptor, cargo and Ran–GTP for stable complex formation[25–28].

Our data indicate a model that may explain how localization of Pho4 is regulated by phosphorylation (Fig. 4c). In high-phosphate medium, the activated Pho80–Pho85 cyclin–CDK complex phosphorylates Pho4 in the nucleus, triggering association between phosphorylated Pho4, the export receptor Msn5 and Gsp1–GTP. This trimeric complex is then rapidly exported from the nucleus. By analogy to what has been shown for the other export receptors[25–28], we propose that the Pho4–Msn5–Gsp1–GTP complex is disassembled in the cytoplasm by hydrolysis of GTP by Gsp1, stimulated by Rna1 (yeast RanGAP, a GTPase-activating protein) and Yrb1 (yeast RanBP1, a Ran-binding protein). Phosphorylated cytoplasmic Pho4 is then prevented from re-entering the nucleus because phosphorylation of Pho4 inhibits interaction with the import receptor Pse1 (ref. 14). We have determined that the phosphorylation sites necessary and sufficient for regulating export are distinct from the site that regulates Pho4 import (E.K.O. *et al.*, manuscript in preparation). The dual role for phosphorylation in promoting export and preventing re-import is likely to be a general mechanism, as it allows cells to rapidly and efficiently regulate gene expression in response to environmental signals.

The ability of Msn5 to preferentially recognize phosphorylated Pho4 may be explained in two ways. The Msn5-binding site present on phosphorylated Pho4 could be revealed by a phosphorylation-induced conformational change. Alternatively, Msn5 may recognize a phosphopeptide within Pho4. In this case, Msn5 may also function as an export receptor for other phosphorylated proteins. The existence of an export receptor dedicated to phosphorylated cargo would provide a simple mechanism for selectively exporting proteins that are phosphorylated in response to cellular signals.

Although many proteins are regulated by phosphorylation-induced export from the nucleus, the molecular mechanism by which phosphorylation induces nuclear export has not been understood previously. Our results reveal a new pathway for nuclear export that uses an export receptor that requires only Ran–GTP to bind exclusively to the phosphorylated form of its cargo. These results provide a paradigm for understanding how phosphorylated proteins are exported from the nucleus. □

Methods

Plasmids and strains. *PHO4*, *PHO80* and *PHO85* were deleted in strain K699 (*MAT**a** ade2-1 trp1-1 can1-100 leu2-3,112 his3-11,15 ura3*) and *MSN5* and *PHO4* were deleted in strain IH3195 (*MAT**a** HML**a** HMR**a** ura3-52 ade2-101 met1 leu2Δ1 trp1Δ99*), which is isogenic to JC2-1B (ref. 30), by standard gene replacement. *nup49-313* and the isogenic *NUP49*$^{+}$ strain[16,18], and *nsp1*^{ts} and its isogenic strain[16,17] have been described previously. High-phosphate cultures were grown in standard synthetic dropout (SD) medium; low-phosphate cultures were grown in phosphate-depleted SD medium; and no-phosphate cultures were grown in SD medium with KCl replacing KH_2PO_4 (ref. 14). The construction of plasmids expressing Pho4^{WT} and Pho4^{SA} fused to either GFP or to the zz tag from Protein A, and of the plasmid expressing Myc–Gsp1, has been described[14]. Pho80–GFP and Pho85–GFP were expressed from their own promoter on a high-copy or low-copy plasmid, respectively. Both plasmids complement the phenotype of the respective deletion strain. Detailed descriptions of plasmids used in this study are available on request.

Detection of phosphorylation of Pho4–zz. Isogenic *pho4Δ* and *pho4Δmsn5Δ* strains expressing Pho4^{WT}–zz from a plasmid were inoculated at an A_{600} value of 0.1–0.3 and grown in low-phosphate medium for 8 h. Cells were collected 10 min after the addition of KH_2PO_4 or KCl to a final concentration of 20 mM and were frozen in liquid nitrogen. Samples were lysed by boiling for 5 min in the presence of SDS–PAGE loading buffer followed by bead-beating with acid-washed 0.5-mm glass beads for 5 min. Samples were reboiled for 3 min and 10–15 μg total protein was separated using 7.8% SDS–PAGE and immunoblotted to detect the zz tag.

Phosphate starvation and microscopy. Phosphate starvation and microscopy were done as described[14], except that the photographs for Fig. 2 were taken using an Olympus PM-30 camera.

Examination of Pho4^{WT}–GFP in the *nsp1*^{ts} strain. The *nsp1*^{ts} strain carrying a plasmid expressing Pho4^{WT}–GFP was starved for phosphate for 4–8 h in low-phosphate medium at 23 °C, resulting in the accumulation of Pho4^{WT}–GFP in the nucleus. Cells were then shifted to 38.5 °C for 4–6 h to impair protein import. Cycloheximide was added to a final concentration of 0.1 mg ml^{-1} and the culture was incubated for 10 min. For the phosphate-containing samples, 4.5 μl culture plus 0.5 μl of 15 mg ml^{-1} KH_2PO_4 were mixed on a slide and Pho4–GFP localization was examined by direct fluorescence. Similar results were obtained with the *nup49-313* strain (data not shown).

Expression and purification of recombinant proteins. Msn5 was expressed in *Escherichia coli* with a His_6 tag at the carboxy terminus essentially as described for Pse1–His_6 (ref. 14), with the following modifications: cells were lysed in lysis buffer containing 10 mM imidazole and Msn5–His_6 was eluted with a 10–1,000 mM imidazole gradient. Myc–Gsp1, Pho4^{WT}–zz and Pho4^{SA}–zz were expressed and purified as described[14]. RanQ69L was expressed in strain BL21 grown at 37 °C in Luria broth + 100 μg ml^{-1} carbenicillin to an A_{600} value of 0.4 and induced with 0.4 mM isopropyl-β-D-thiogalactoside at 30 °C for 1.5 h. RanQ69L was purified as reported for Myc–Gsp1 (ref. 14).

Binding assay. *In vitro* phosphorylation of Pho4–zz and loading of Myc–Gsp1 with GTP or GDP were done as described[14]. Yeast whole cell extract was prepared nearly as described[14] except that phosphatase inhibitors were included (80 mM β-glycerophosphate, 10 mM NaF, 10 nM calyculin A). Binding of Myc_3–Msn5 to Pho4–zz was essentially as described for Pse1 (ref. 14), with the following modifications: first, purified RanQ69L was added to a final concentration of 5 μM; second, an ATP-regenerating system was added (1 mM ATP, 1 mM GTP, 50 μg ml^{-1} creatine kinase, 5 mM creatine phosphate); and third, phosphatase inhibitors were reduced to 40 mM β-glycerophosphate, 5 mM NaF and 5 nM calyculin A. Binding with purified components was done by incubating 25 μg purified Pho4–zz immobilized on IgG–Sepharose beads with a final concentration of 1 μM Myc–Gsp1 and 1 μM Msn5–His_6 in the presence of 0.5 mg ml^{-1} bovine serum albumin for 1.5 h at 4 °C.

Received 15 September; accepted 15 October 1998.

1. Nigg, E. A. Nucleocytoplasmic transport: signals, mechanisms and regulation. *Nature* **386,** 779–787 (1997).
2. Jans, D. A. & Hubner, S. Regulation of protein transport to the nucleus: central role of phosphorylation. *Physiol. Rev.* **76,** 651–685 (1996).
3. Timmerman, L. A., Clipstone, N. A., Ho, S. N., Northrop, J. P. & Crabtree, G. R. Rapid shuttling of NF-AT in discrimination of Ca^{2+} signals and immunosuppression. *Nature* **383,** 837–840 (1996).
4. Shibasaki, F., Price, E. R., Milan, D. & McKeon, F. Role of kinases and the phosphatase calcineurin in the nuclear shuttling of transcription factor NF-AT4. *Nature* **382,** 370–373 (1996).
5. De Vit, M. J., Waddle, J. A. & Johnston, M. Regulated nuclear translocation of the Mig1 glucose repressor. *Mol. Biol. Cell* **8,** 1603–1618 (1997).
6. Gorner, W. *et al.* Nuclear localization of the C2H2 zinc finger protein Msn2p is regulated by stress and protein kinase A activity. *Genes Dev.* **12,** 586–597 (1998).
7. Fornerod, M. *et al.* The human homologue of yeast CRM1 is in a dynamic subcomplex with CAN/Nup214 and a novel nuclear pore component Nup88. *EMBO J.* **16,** 807–816 (1997).
8. Gorlich, D. *et al.* A novel class of RanGTP binding proteins. *J. Cell Biol.* **138,** 65–80 (1997).
9. Kaffman, A., Herskowitz, I., Tjian, R. & O'Shea, E. K. Phosphorylation of the transcription factor PHO4 by a cyclin–CDK complex, PHO80–PHO85. *Science* **263,** 1153–1156 (1994).
10. O'Neill, E. M., Kaffman, A., Jolly, E. R. & O'Shea, E. K. Regulation of PHO4 nuclear localization by the PHO80–PHO85 cyclin–CDK complex. *Science* **271,** 209–212 (1996).

11. Oshima, Y. The phosphatase system in *Saccharomyces cerevisiae*. *Genes Genet. Syst.* **72,** 323–334 (1997).
12. Ogawa, N. *et al.* Functional domains of Pho81p, an inhibitor of Pho85p protein kinase, in the transduction pathway of Pi signals in *Saccharomyces cerevisiae*. *Mol. Cell. Biol.* **15,** 997–1004 (1995).
13. Schneider, K. R., Smith, R. L. & O'Shea, E. K. Phosphate-regulated inactivation of the kinase PHO80–PHO85 by the CDK inhibitor PHO81. *Science* **266,** 122–126 (1994).
14. Kaffman, A., Rank, N. M. & O'Shea, E. K. Phosphorylation regulates association of the transcription factor Pho4 with its import receptor Pse1/Kap121. *Genes Dev.* **12,** 2673–2683 (1998).
15. Lee, M. S., Henry, M. & Silver, P. A. A protein that shuttles between the nucleus and the cytoplasm is an important mediator of RNA export. *Genes Dev.* **10,** 1233–1246 (1996).
16. Wimmer, C., Doye, V., Grandi, P., Nehrbass, U. & Hurt, E. C. A new subclass of nucleoporins that functionally interact with nuclear pore protein NSP1. *EMBO J.* **11,** 5051–5061 (1992).
17. Nehrbass, U. *et al.* NSP1: a yeast nuclear envelope protein localized at the nuclear pores exerts its essential function by its carboxy-terminal domain. *Cell* **61,** 979–989 (1990).
18. Doye, V., Wepf, R. & Hurt, E. C. A novel nuclear pore protein Nup133p with distinct roles in poly(A)$^+$ RNA transport and nuclear pore distribution. *EMBO J.* **13,** 6062–6075 (1994).
19. Aitchison, J. D., Blobel, G. & Rout, M. P. Kap104p: a karyopherin involved in the nuclear transport of messenger RNA binding proteins. *Science* **274,** 624–627 (1996).
20. Xiao, Z., McGrew, J. T., Schroeder, A. J. & Fitzgerald-Hayes, M. CSE1 and CSE2, two new genes required for accurate mitotic chromosome segregation in *Saccharomyces cerevisiae*. *Mol. Cell. Biol.* **13,** 4691–4702 (1993).
21. Stade, K., Ford, C. S., Guthrie, C. & Weis, K. Exportin 1 (Crm1p) is an essential nuclear export factor. *Cell* **90,** 1041–1050 (1997).
22. Seedorf, M. & Silver, P. A. Importin/karyopherin protein family members required for mRNA export from the nucleus. *Proc. Natl Acad. Sci. USA* **94,** 8590–8595 (1997).
23. Rout, M. P., Blobel, G. & Aitchison, J. D. A distinct nuclear import pathway used by ribosomal proteins. *Cell* **89,** 715–725 (1997).
24. Kadowaki, T. *et al.* Isolation and characterization of *Saccharomyces cerevisiae* mRNA transport-defective (mtr) mutants. *J. Cell Biol.* **126,** 649–659 (1994).
25. Arts, G. J., Fornerod, M. & Mattaj, I. W. Identification of a nuclear export receptor for tRNA. *Curr. Biol.* **8,** 305–314 (1998).
26. Kutay, U., Bischoff, F. R., Kostka, S., Kraft, R. & Gorlich, D. Export of importin alpha from the nucleus is mediated by a specific nuclear transport factor. *Cell* **90,** 1061–1071 (1997).
27. Kutay, U. *et al.* Identification of a tRNA-specific nuclear export receptor. *Mol. Cell* **1,** 359–369 (1998).
28. Fornerod, M., Ohno, M., Yoshida, M. & Mattaj, I. W. CRM1 is an export receptor for leucine-rich nuclear export signals. *Cell* **90,** 1051–1060 (1997).
29. Bischoff, F. R., Klebe, C., Kretschmer, J., Wittinghofer, A. & Ponstingl, H. RanGAP1 induces GTPase activity of nuclear Ras-related Ran. *Proc. Natl Acad. Sci. USA* **91,** 2587–2591 (1994).
30. Chenevert, J., Valtz, N. & Herskowitz, I. Identification of genes required for normal pheromone-induced cell polarization in *Saccharomyces cerevisiae*. *Genetics* **136,** 1287–1296 (1994).

Acknowledgements. We thank I. Herskowitz, J. Li, J. Weissman and members of the O'Shea laboratory for comments on the manuscript; R. Bischoff for the RanQ69L plasmid; M. Lenburg for the Pho85–GFP plasmid; and J. Aitchison, K. Weis, P. Silver, M. Fitzgerald-Hayes, E. Hurt and A. Tartakoff for yeast strains. A.K. is a Fellow of the UCSF Medical Scientist Training Program. N.M.R. and L.S.H. were supported by fellowships from the NIH and E.M.O. was supported by a fellowship from the Jane Coffin Childs Foundation. This work was supported by the David and Lucile Packard Foundation and by an NSF Presidential Faculty Fellowship (E.K.O.).

Correspondence and requests for materials should be directed to E.K.O. (e-mail: oshea@biochem.ucsf.edu).

Crystal structure of the ligand-binding domain of the receptor tyrosine kinase EphB2

Juha-Pekka Himanen*, Mark Henkemeyer† & Dimitar B. Nikolov*

** Cellular Biochemistry and Biophysics Program, Memorial-Sloan-Kettering Cancer Center, 1275 York Avenue, New York, New York 10021, USA*
† Center for Developmental Biology, University of Texas Southwestern Medical Center, Dallas, Texas 75235-9133, USA

The Eph receptors, which bind a group of cell-membrane-anchored ligands known as ephrins, represent the largest subfamily of receptor tyrosine kinases (RTKs)[1]. They are predominantly expressed in the developing and adult nervous system[2] and are important in contact-mediated axon guidance[3–6], axon fasciculation[5,7] and cell migration[8–11]. Eph receptors are unique among other RTKs in that they fall into two subclasses with distinct ligand specificities[12], and in that they can themselves function as ligands to activate bidirectional cell–cell signalling[4,13,14]. We report here the crystal structure at 2.9 Å resolution of the amino-terminal ligand-binding domain of the EphB2 receptor (also known as Nuk)[15–17]. The domain folds into a compact jellyroll β-sandwich composed of 11 antiparallel β-strands. Using structure-based mutagenesis, we have identified an extended loop that is important for ligand binding and class specificity. This loop, which is conserved within but not between Eph RTK subclasses, packs against the concave β-sandwich surface near positions at which missense mutations cause signalling defects[18], localizing the ligand-binding region on the surface of the receptor.

The extracellular region of Eph receptors consists of two fibronectin type III repeats, a cysteine-rich region, and a conserved 180-amino-acid N-terminal 'globular' domain (Fig. 1) which is both necessary and sufficient for bindings of the receptors to their ephrin ligands[16]. Eph receptors bind their ephrin ligands with high affinity ($K_d = 0.5–15.0$ nM) and with one-to-one stoichiometry[16,17,19] (Fig. 2).

We determined the structure of the biologically active (Fig. 2) ligand-binding domain of the murine EphB2 receptor by X-ray crystallography using the multiple isomorphous replacement (MIR) method (Table 1 and Figs 3, 4). Our model is refined at 2.9 Å resolution to an *R*-factor of 20.6% with tightly restrained temperature factors and good stereochemistry. The domain has dimensions of roughly 50 Å × 40 Å × 30 Å. It has two antiparallel β-sheets, with the usual left-handed twist, packed against each other to form a compact β-sandwich, and a short 3_{10} helix. The concave β-sheet is composed of strands C, F, F′ L, H and I, and the convex β-sheet of strands D, E, A, M, G, K and J (Fig. 4c). The extensive hydrophobic core created by approximation of the two β-sheets and the short 3_{10} helix contains no cavities and is dominated by aromatic side chains. The β-strands are connected by loops of varying length, including a long loop (between strands H and I; coloured in orange and red in Fig. 4a) that packs against the full width of the concave β-sheet, and two loops (D–E and J–K) that protrude from the two sides of the β-sandwich, closing on the middle of the convex β-sheet. The H–I loop (in the front in Fig. 4a) is well-ordered, as are the loops running across the top, whereas the D–E and J–K loops at the back are disordered, with several residues that cannot be located in the electron-density map. Two disulphide bridges stabilize the loops at the top of the β-sandwich: Cys 105 binds Cys 115 in the longest of the top loops (G–H), and Cys 70, the first residue of loop E–F, binds Cys 192, the last residue of loop L–M.

The EphB2 ligand-binding domain has a jellyroll folding topology[20] (Fig. 4c). Comparison of this structure with the contents of the FSSP database[21] reveals considerable similarity with the carbohydrate-binding domains of glucanases, legume lectins, β-galactosidases, sialidases, cellulases, bacterial toxins and influenza virus haemagglutinin. This raises two interesting possibilities, namely that the homology in molecular architecture includes the location of the ligand-binding site, or that the carbohydrate moieties at the putative glycosylation sites of the ephrins[3] are directly involved in ligand–receptor recognition. Our results support the first possibility (see below); however, we suggest that the Eph receptors are not lectins. Indeed, the purified EphB2 globular domain forms a stable, high-affinity complex with a bacterially expressed non-glycosylated ephrin-B2 ligand preparation (Fig. 2) (K_d is within the range of values reported for recombinant glycosylated ephrins[2,16,17,19]). Furthermore, addition of a tenfold molar excess of *N*-linked type oligosaccharides (Oxford GlycoSystem) has no effect on the *in vitro* Eph-receptor–ephrin interaction (data not shown). Beyond the similarity in overall topology between the EphB2 ligand-binding domain and the carbohydrate-binding proteins, the precise structures are quite different (Fig. 4d) and the best structural alignments include stretches of 100–120 amino acids with root mean square deviations between α-carbon positions of 3.0 Å.

The ligand-binding domain of Eph receptors is unique to this family of RTKs[22] and shares no significant amino-acid-sequence homology with other known proteins. Nevertheless, jellyroll folding topology is observed in the extracellular domains of other proteins including, in addition to the carbohydrate-binding proteins, the tumour-necrosis factor (TNF) family[23] (which includes TNF, lym-